16TH EUROPEAN CONFERENCE ON EARTHQUAKE ENGINEERING THESSALONIKI 18 - 21 JUNE 2018

SEISMIC FRAGILITY ANALYSIS OF RC FRAMES WITH MASONRY INFILLS

Hossameldeen MOHAMED[1], Xavier ROMÃO[2]

ABSTRACT

Given the evidence provided by past earthquakes and experimental tests carried out since the mid-1950s, the contribution of the infill wall on the global response of the RC structures cannot be ignored. Therefore, the seismic vulnerability of this type of buildings needs to be assessed by considering the effect of the infill wall to determine their level of safety and, therefore, to identify their possible strengthening needs. This paper addresses the seismic fragility assessment of several reinforced concrete (RC) frames with different infill panel configurations and number of storeys. The selected structures involve fully infilled and partially infilled RC frames, as well as RC frames with an open ground floor, with four and eight storeys, whose behaviour was compared to that of the corresponding bare frames. The behaviour of the infill panel was simulated by a single strut model with properties that were calibrated using experimental data. Each structure was analysed using nonlinear dynamic analysis considering fifty real ground motion records that were scaled to several intensities. Structural performance was measured using maximum interstorey drifts over the height of the structure and fragility curves were then computed based on the demand distributions for several limit states. The fragility curves that were obtained show distinctive evolutions reflecting the different behaviour of the selected structures due to their infill configurations.

Keywords: Infilled RC frames; masonry infills; fragility curve; interstorey drift

1. INTRODUCTION

Infilled reinforced concrete (RC) frames are one of the most common structural systems around the world. Most of these structures were built without considering the effect of the masonry infills on the behaviour of the structures under earthquake loads. However, evidence from past earthquakes (e.g. see (Romão et al. 2013, Ohsumi et al. 2016, Shakya and Kawan 2016)), showed that these infilled structures have a different behaviour in terms of failures modes when compared to that of the corresponding bare frames. In addition, experimental tests carried out since the mid-1950s (e.g. see Polyakov (1956), (Zarnic and Tomazevic 1988) (Bergami 2007, Zhai et al. 2016) among others) show that, in some cases, infills can lead to premature failure while in others they can improve the actual performance of the building. Based on these observations, it is clear that the contribution of the infill to the structural behaviour should not be neglected. These facts imply the need to assess the seismic vulnerability of this type of buildings considering the masonry contribution in order to determine their level of safety and, therefore, to identify their possible strengthening needs. In this context, this paper presents a study addressing the seismic fragility assessment of several 2D RC frames with different infill panel configurations and number of storeys. The selected structures involve fully infilled, partially infilled frames and frames with an open ground floor, with four and eight storeys, whose behaviour will be compared to that of the corresponding bare frames. Since fragility functions are increasingly used in the modern performance-based evaluation of structures to relate the seismic hazard of the site to the probability of exceedance of a given limit state of the structure, a detailed analysis addressing the development of fragility functions for different limit states was carried out for the considered case-studies. The fragility curves were developed using incremental dynamic analysis (IDA) (Vamvatsikos and Cornell 2002), a computational analysis procedure for performing a comprehensive assessment of

[1]Assistant Professor, Faculty of engineering, Aswan university, Aswan, Egypt, Hossam.ahmed@aswu.edu.eg
[2]Assistant Professor, Department of Civil engineering, CONSTRUCT-LESE, Faculty of Engineering, University of Porto, Porto, Portugal, xnr@fe.up.pt

the behaviour of structures under seismic loading. The IDA curves were developed by incrementing the intensity of fifty real ground motion records selected to match a target response spectrum and to cover a wide range of structural behaviour levels up to collapse. The selected target response spectrum defining the reference seismic scenario corresponds to that of Zone 3 of the Portuguese territory considering the interplate seismic action (type 1) and a soil of type B according to the Portuguese National Annex of Eurocode 8 (EC8-1, 2010). With respect to the infill modelling, the behaviour of the infills was simulated using a single strut model whose properties were calibrated using experimental data to reduce its uncertainty. In order to trace the contribution of the infills for several damage states, fragility curves were determined for six different limit states defined in terms of maximum interstorey drift over the height of the structure.

2. CHARACTERISTICS OF THE CONSIDERED BUILDINGS

In order to assess the effect of the infill panels on the vulnerability of RC buildings, an office building was selected to be a representative case study. An overall description of the building configurations and general characteristics that were considered to define the RC frames structures that were analysed is presented in the following. The selected RC frames are considered to be part of office buildings whose architectural plan view of the typical floor is presented in Figure 1 a) while the structural system of the typical floor is presented in Figure 1 b). The frame of the vertical axis 5 between the horizontal axes A-D, termed herein as frame F5A-D, is the considered frame for the vulnerability analysis. This frame was analysed with different configurations (bare, fully infilled, soft-storey and partially infilled frames) and with two different numbers of storeys (four and eight storeys) as shown in Figure 2 and Figure 3, respectively.

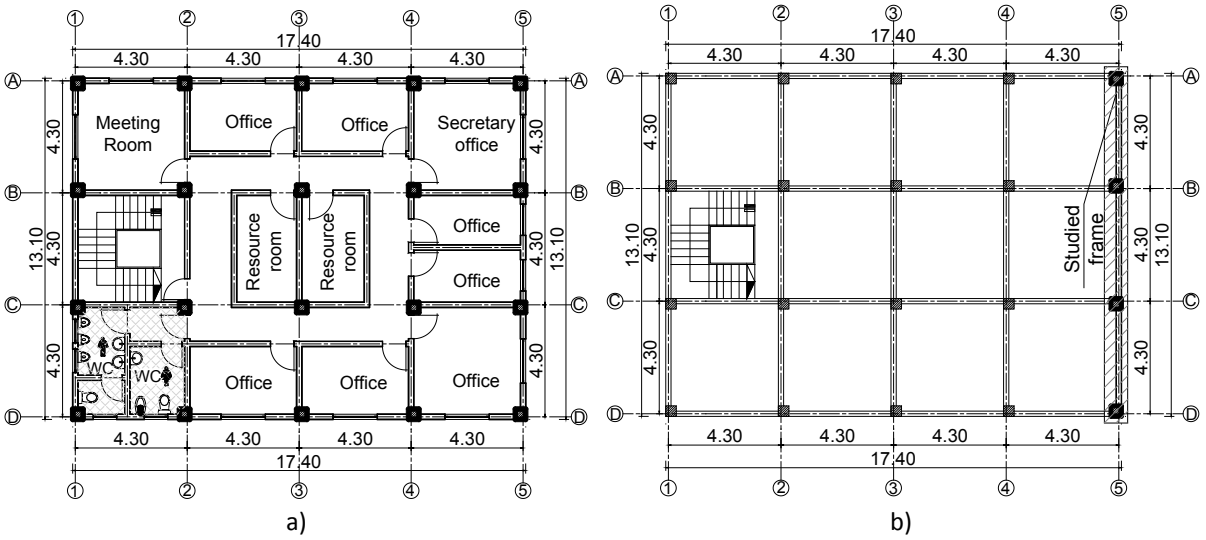

Figure 1 Typical plan view for the considered office building: a) architectural plan b) structural system showing the considered frame (all dimensions in m)

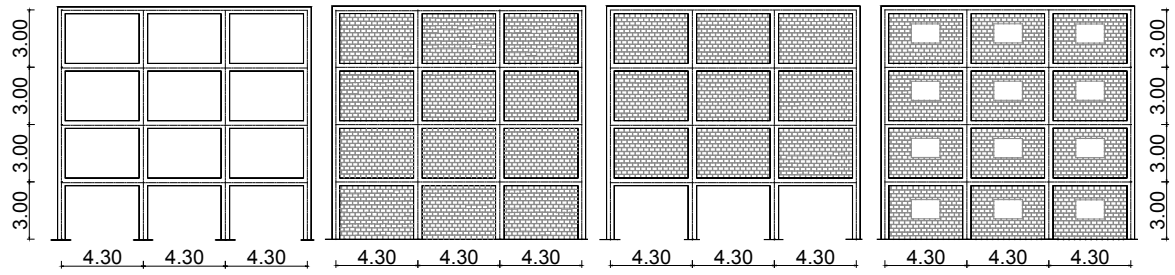

a) Bare frame BF-4 *b) Fully infilled FF-4* *c) Soft storey frame SF-4* *d) Partially infilled PF-4*

Figure 2 Different frame configurations for the four-storey building (all dimensions in m)

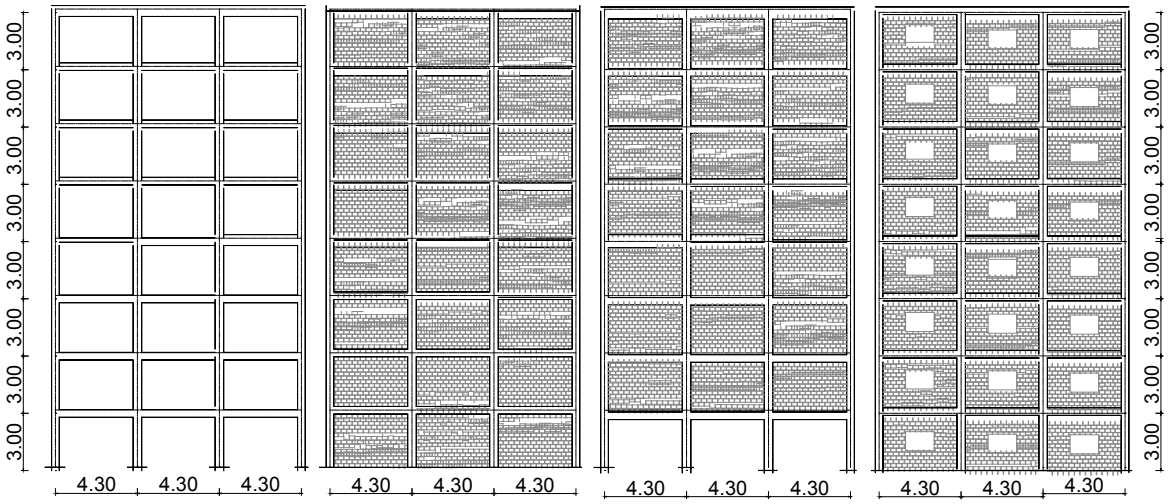

a) Bare frame BF-8 *b) Fully infilled FF-8* *c) Soft storey frame SF-8* *d) Partially infilled PF-8*

Figure 3 Different frame configurations for the eight-storey building (all dimensions in m)

The structures were designed for gravity loading only to represent a scenario of non-seismically designed structures. The mechanical properties of the selected materials are presented in Table 1 and the cross-section details for frame F5A-D are shown in Table 2. It is noted that the reinforcement details were homogenised in order to have a small number of different cross sections. The infills were defined according to the data from the experimental campaign of (Kakaletsis and Karayannis 2009). The size and configurations of the infill panels were scaled to match the real size of the building while maintaining the aspect ratio of the panels equal to that of the test panels.

Table 1 Mechanical properties of the materials

Concrete compressive strength f_c (MPa)	**Steel**		**Infill panel material**	
	Yield stress σ_y (MPa)	Elastic modulus (GPa)	Brick unit compressive strength f_m (MPa)	Mortar compressive strength f_{mo} (MPa)
25.0	522.0	190.0	3.1	1.53

Table 2 Cross-section details for frame F5A-D

No of storeys	**Axis**	**Columns**			**Beams**					
					Reinforcement					
		Section (cm^2)	**Steel**	**Section (cm^2)**	**Start**		**Middle**		**End**	
					upper	**lower**	**upper**	**lower**	**upper**	**lower**
Four storeys	A	30x30	8 Ø15	25x40	4 Ø12	4 Ø12	4 Ø12	4 Ø12	4 Ø12	4 Ø12
	B	30x30	8 Ø15	25x40	4 Ø12	4 Ø12	4 Ø12	4 Ø12	4 Ø12	4 Ø12
	C	30x30	8 Ø15	25x40	4 Ø12	4 Ø12	4 Ø12	4 Ø12	4 Ø12	4 Ø12
	D	30x30	8 Ø15	25x40	4 Ø12	4 Ø12	4 Ø12	4 Ø12	4 Ø12	4 Ø12
Eight storeys	A	30x30	8 Ø15	25x40	4 Ø12	4 Ø12	4 Ø12	4 Ø12	4 Ø12	4 Ø12
	B	45x45	10 Ø15	25x40	4 Ø12	4 Ø12	4 Ø12	4 Ø12	4 Ø12	4 Ø12
	C	45x45	10 Ø15	25x40	4 Ø12	4 Ø12	4 Ø12	4 Ø12	4 Ø12	4 Ø12
	D	30x30	8 Ø15	25x40	4 Ø12	4 Ø12	4 Ø12	4 Ø12	4 Ø12	4 Ø12

3. NUMERICAL MODEL DESCRIPTION

The software OpenSees (McKenna et al. 2000) was used to perform the nonlinear dynamic analyses for all the considered numerical models. The RC frame elements (i.e. beams and columns) were modelled using the force-based element known as the beam with hinges with the nonlinear behaviour of the hinges represented by fibre-sections. The Modified Radau Hinge Integration method (Fenves and Scott 2006, Scott and Ryan 2013) was the selected plastic hinge integration method to assign inelastic actions at the

end regions of the element with a specified length. Additional fibre sections were also considered in the central part of the element to model its possible nonlinearity (Scott, *et al.*, 2013). A total of six integration points are used in the element state determination (two for each hinge and two for the central part of the element). The value of the plastic hinge length l_p was defined by the following expression proposed by Paulay and Priestley (1992):

$$l_p = 0.08l_e + 0.022d_b f_y \quad (1)$$

where l_e is the element length, d_p is the diameter of the steel rebars and f_y is the steel yield stress in MPa. For the fibre discretization of the RC cross sections, the concrete cover was modelled using the concrete model termed Concrete01 representing the uniaxial concrete material with no tensile strength and a degraded linear unloading/reloading stiffness in compression. Confined concrete was modelled using a confinement factor determined based on the expression proposed by Kent and Park (1971) associated with the Concrete01 model. Steel reinforcement bars were modelled using the uniaxial Giuffre-Menegotto-Pinto model (Menegotto and Pinto 1973) with isotropic hardening, termed Steel02 in OpenSees, with the default parameters proposed by the software. For the beam-column joints, a rigid end-offset joint model was used (Mondal and Jain 2008). The lengths of the rigid parts were considered to be half of the depth of the perpendicular element.

The infills were modelled using a single compressive strut element connected to the RC frame at the corner nodes. The properties of the strut element were determined using the stiffness-based approach where the cross-section of the strut was defined and a constitutive model for the masonry was used to simulate the nonlinear behaviour of the infill. The referred properties were optimized to match the experimental data of specimens S (solid panel) and specimen WO3 (partially infilled panel) from the test campaign of (Kakaletsis and Karayannis 2008). Although the selected specimens were tested with a reduced scale factor, the extracted responses of the infill were scaled according to the ratio between the tested panel and the panel considered in the numerical models which has the same aspect ratio of the scaled panel (CEB 1996, Petry and Beyer 2014). Figure 4 shows the general description of the model implemented in OpenSees for the RC frame and the infill panel in addition to the detailed description of the RC element model.

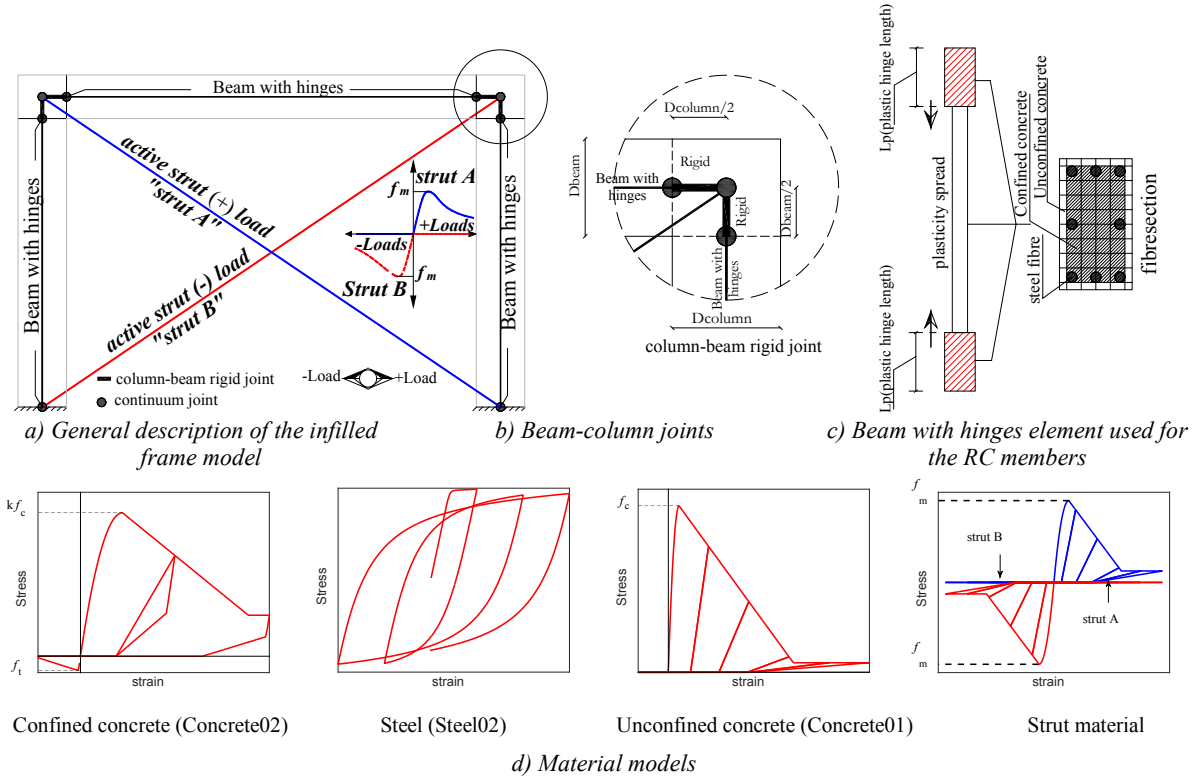

a) General description of the infilled frame model *b) Beam-column joints* *c) Beam with hinges element used for the RC members*

d) Material models

Figure 4 Description of the implemented model for the infill panel using a stiffness-based approach.

To complement the description of the models, the fundamental periods of the considered frames with different configurations were determined from modal analyses. Table 3 presents the periods of the first and second modes of the four- and eight-storey bare and infilled frames. By comparing the values presented in the referred table, it is clear that considering the contribution of the infills introduces a significant reduction of the fundamental periods of the structures and, therefore, a significant change of their dynamic characteristics, as will be presented throughout this paper.

Table 3 First and second mode periods of the considered structures

No. of storeys	Model	Acronym	T_1 (s)	T_2 (s)
Four storeys	Bare frame	BF-4	0.68	0.22
	Fully infilled	FF-4	0.21	0.07
	Soft storey infilled	SF-4	0.44	0.9
	Partially frame	PF-4	0.23	0.08
Eight storeys	Bare frame	BF-8	1.05	0.35
	Fully infilled	FF-8	0.45	0.15
	Soft storey infilled	SF-8	0.57	0.19
	Partially frame	PF-8	0.47	0.17

4. METHODOLOGY OF THE FRAGILITY ANALYSIS

Incremental dynamic analysis (IDA) was selected to assess the performance of the considered structures. IDA is a computational procedure for performing a comprehensive assessment of the behaviour of structures under seismic loading. The procedure involves subjecting a structural model to one or more ground motions, each scaled to multiple levels of intensity, to produce one or more curves of structural response versus the ground motion intensity levels (Vamvatsikos and Cornell 2002). Therefore, performing a multi ground motion IDA that will capture the response uncertainty coming from the record-to-record variability requires a series of nonlinear dynamic analyses under a suite of adequate ground motion records scaled multiple times. The scaling levels need to be appropriately selected to obtain the structure's response throughout its entire range of behaviour. Furthermore, the ground motion scaling levels reflect increasing levels of the ground motion intensity that is defined by a parameter usually termed intensity measure (IM).

The structure's response (or demand) can be defined by any type of structural or non-structural parameter, local or global (e.g. maximum interstorey drift over the height, peak storey drifts, peak floor accelerations, shear force, chord rotation, etc). In this study, the maximum interstorey drift over the height is considered as the structural demand parameter representing the behaviour of the structures. This demand parameter was selected due to its good correlation with structural losses and with a large part of non-structural losses. With respect to the selected IM, even though the 5%-damped spectral acceleration for the first-mode period of the structure is one of the most widely used IMs, due to the variability of the first mode period of the structures during its range of behaviour (e.g. depending on whether the infill is active or not, or depending on the level of ductility demand), the peak ground acceleration (PGA) was considered instead. Furthermore, considering PGA also allows for a more direct comparison of the fragility curves between the structures since the same IM is common to all structures. The IDAs of each structure were determined using fifty real ground motion records that match the selected target response spectrum. The selected target response spectrum defining the reference seismic scenario corresponds to that of Zone 3 of the Portuguese territory considering the interplate seismic action (type 1) and a soil of type B according to the Portuguese National Annex of Eurocode 8 (EC8-1, 2010). The PGA considered for this scenario was 0.15g, corresponding to a return period of 475 years. The records were selected from the NGA database (Chiou et al. 2008) using the software SelEQ (Macedo et al. 2013, Araújo et al. 2016). These records were selected by optimizing the match between the average response spectrum of the records and the target spectrum in the range of periods between 0.15s and 1.5s, which covers all fundamental periods of the selected structures (Ricci et al. 2016). Furthermore, the ground motion selection process also ensures that, for this period range, the spectral values of each individual ground motion are within a bound defined by ±50% of the target spectral values. Figure 5 shows the elastic response spectrum for the fifty ground motion records along with their

mean spectrum and the target response spectrum. As referred before, the selected IM was PGA and each ground motion was scaled to several intensities starting from 0.05g until an intensity that leads to global dynamic instability (i.e. "numerical failure").

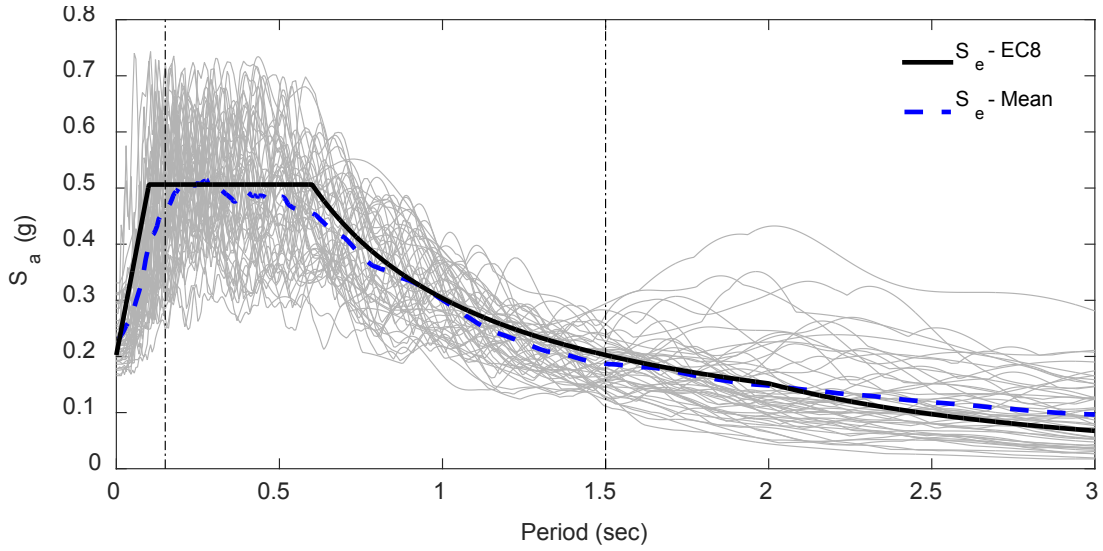

Figure 5 Scaled response spectra for the fifty ground motions with their mean response spectrum and the target elastic response spectrum for Zone 3 of the Portuguese territory (type 1 earthquake and soil B)

In the present paper, since structural demand and performance is defined in terms of maximum interstorey drifts over the height of the structure (IDRmax), the limit states shown in Table 4 were used, which correspond to those proposed by (Rossetto and Elnashai 2005). Furthermore, fragility curves were obtained using an IM-based approach (Ibarra et al. 2002)

Table 4 Threshold values for the considered damage limit states defined in terms of IDR_{max}

Damage state	Slight damage	Light damage	Moderate damage	Extensive damage	Partial collapse	Collapse
IDR (%)	0.05	0.08	0.30	1.15	2.80	>4.36

5. RESULTS OF THE FRAGILITY ANALYSES AND DISCUSSION

The empirical fragility data and the fragility curves that were obtained assuming they can be represented by the lognormal distribution are presented in Figure 6 for the several four-storey structures and for the six different limit states. As can be seen, the lognormal distribution appears to provide an overall good fit to the fragility data. With respect to the performance of the structures, PF- and FF-4 exhibit better performance for all the limit states. Furthermore, the SF-4 structure can be seen to be the one exhibiting the worst performance among all configurations, especially for higher damage limit states. The fact that the BF-4 and SF-4 structures reach almost any level of damage for lower intensities can be explained by the non-seismically designed RC elements controlling their behaviour combined with the fact that the infills act as behaviour modifiers for the PF-4 and FF-4 structures enhancing their performance for the less severe limit states. As can be seen, for the first three limit states (i.e. slight, light and moderate damage), BF-4 and SF-4 have a close performance while the performance of PF-4 is closer to that of FF-4. After reaching the extensive damage limit state, the BF-4 structure exhibits a better performance than the SF-4 structure due to its higher capacity to spread plasticity. The higher vulnerability of SF-4 for the more severe limit states is a direct result of the soft-storey failure mechanism that is easily reached due to the weak ground storey structural configuration. Furthermore, it is also noted that for the more severe limits states (i.e. the partial collapse and collapse limit states), the performance of PF-4 and FF-4

is closer to that of BF-4 as a result of losing a significant part of the strength after the failure of the infills. For those levels of seismic demand, the behaviour of the PF-4 and FF-4 structures approaches that of the BF-4 structure since most of the infills are inactive.

In a more quantitative analysis, SF-4 and BF-4 can be seen to reach the slight and light damage limit states for PGA values lower than 0.05g while FF-4 and PF-4 require PGA levels higher than 0.15g. Analysing the moderate damage limit state yield similar results between the structures as the BF-4 and SF-4 structures reach this limit state for PGA values lower than 0.13 g while the PF-4 and FF-4 structures exhibit a capacity that can go up to 0.44g. For the extensive damage limit state, the behaviour of the four structures begins to spread and the limit state capacities of SF-4, BF-4, PF-4 and FF-4 can now go up to 0.39g, 0.45g, 1.10g, and 1.25g, respectively. For the partial collapse limit state, the two groups of structures with a distinct behaviour are now much closer as well as their capacities. In this case, the limit state capacities of the SF-4, BF-4, PF-4 and FF-4 structures can go up to 0.9g, 1.4g, 1.6g, and 1.8g, respectively. Finally, for the collapse limit state, the limit states capacities of BF-4, SF-4, PF-4 and FF-4 can go up to 2.7g, 1.2g, 2.1g, and 2.5g, respectively. In this case, it can be seen that BF-4 appears to be able to support higher levels of ground shaking in some cases. However, it can also be seen that, for this limit state, its fragility curve exhibits a much larger variability. With respect to this parameter, it can be seen that, as the severity of the limit state increases, the variability of the performance of the structures also increases, as expected. However, this increase in the variability is more regular for the PF-4 and FF-4 structures than for the SF-4 structure which exhibits a significant increase in the variability of its performance after reaching the extensive damage limit state.

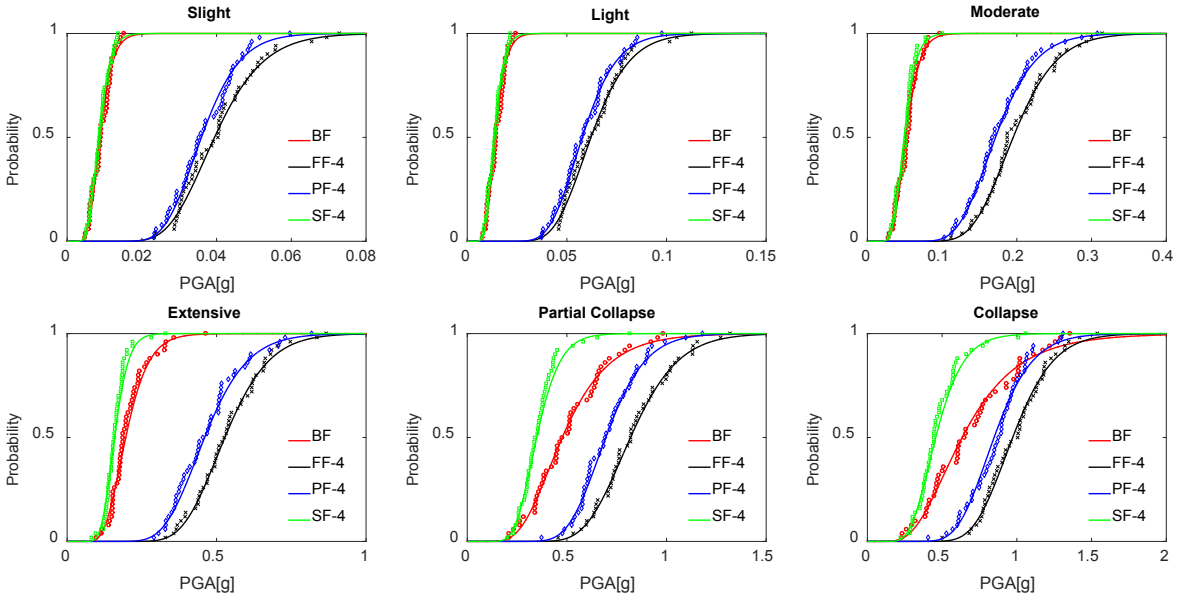

Figure 6 Fragility curves of the several four-storey structures for different limit states

As for the four-storey structures, Figure 7 presents the empirical fragility data and the fragility curves that were obtained assuming they can be represented by the lognormal distribution, for the several eight-storey structures and for the six different limit states. As can be seen, the lognormal distribution also appears to provide an overall good fit to the fragility data. With respect to the performance of the structures, the fragility curves for these structures exhibit a trend similar to that of the four-storey structures: for the lower severity limit states, structures BF-8 and SF-8 exhibit a higher vulnerability than the PF-8 and FF-8 structures, while for limit states of larger severity (i.e. from extensive damage onwards), the PF-8 and FF-8 structures start to exhibit a behaviour closer to that of the BF-8 structure. As referred before, the influence of the infills and of their level of damage introduces a behaviour modifier that changes the behaviour of the PF-8 and FF-8 structures as the ground motion intensity increases. When comparing the maximum PGA involved in the first four limit states (i.e. slight, light,

moderate and extensive damage) for the eight-storey structure with those obtained for the four-storey structures, it can be seen that the latter exhibit a higher capacity than the former. On the other hand, for the remaining limit states the trend is opposite. Furthermore, it is also noted that, on average, the variability of the fragility curves of the eight-storey structures (other than the SF-8 structure) is larger than that of the four-storey structures (other than the SF-4 structure), irrespective of the limit state. The larger redistribution capacity and ability to spread the nonlinear behaviour across a larger number of members in the case of the eight-storey structures with respect to that of the four-storey structures may be a factor leading to this situation.

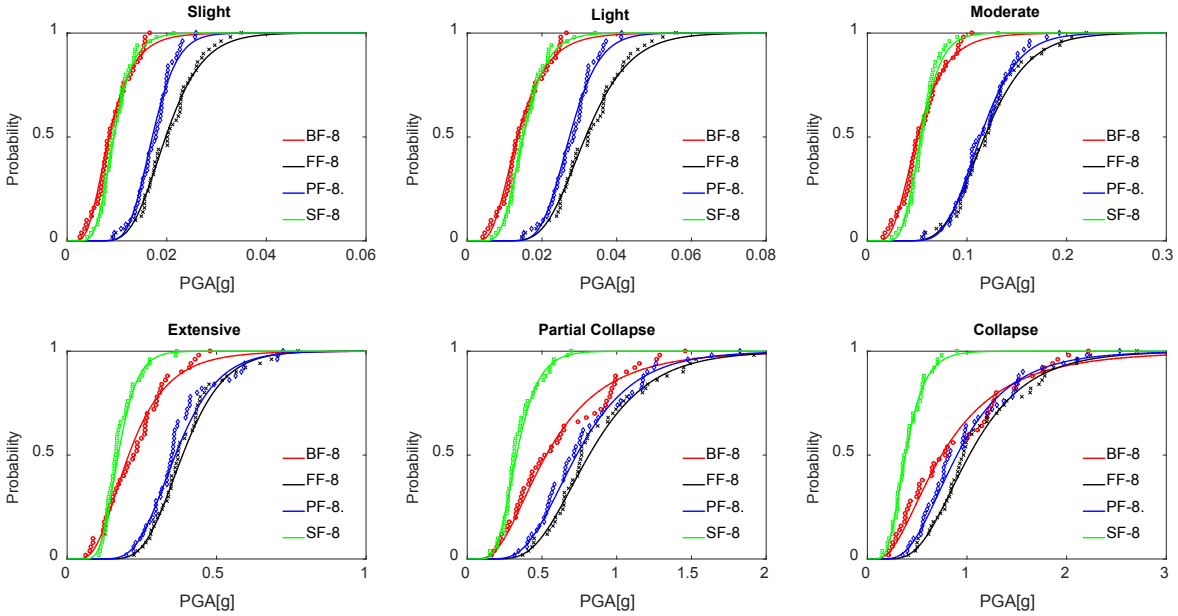

Figure 7 Fragility curves of the several eight-storey structures for different limit states

6. CONCLUSIONS

The seismic vulnerability of RC frames with different configurations of masonry infills was analysed. Configurations involving fully infilled (FF), partially infilled (PF) and soft-storey (SF) structures with four and eight storeys were considered. In addition, the corresponding bare frame model was also analysed and used as a reference case. The behaviour of the structures was analysed by incremental dynamic analysis using fifty real ground motions records. The performance of the structures was then examined for different limit states defined by limits for the maximum interstorey drift over the height of the structure. Performance and vulnerability was then represented by fragility curves obtained using an IM-based approach.

Based on the fragility curves, the performance of the several structures was analysed for the different limit states. For the first three limit states (i.e. slight, light and moderate damage), the four- and eight-storey structures BF and SF have a close performance while the performance of the PF structure is closer to that of the FF structure. After reaching the extensive damage limit state, the BF structure exhibits a better performance than the SF structure due to its higher capacity to spread plasticity. The higher vulnerability of the SF structure for the more severe limit states is a direct result of the soft-storey failure mechanism that is easily reached due to its weak ground storey. Furthermore, for the more severe limits states (i.e. the partial collapse and collapse limit states), the performance of the PF and FF structures is closer to that of the BF structure as a result of losing a significant part of the strength after the failure of the infills.

7. REFERENCES

Araújo, M., L. Macedo, M. Marques and J. M. Castro (2016). "Code-based record selection methods for seismic performance assessment of buildings." *Earthquake Engineering & Structural Dynamics* **45**(1): 129-148.

Bergami, A. V. (2007). Implementation and experimental verification of models for nonlinear analysis of masonry infilled RC frames, Università degli studi ROMA TRE.

CEB (1996). RC frames under earthquake loading: state of the art. London, England, UK, Comité Euro-International du Béton (CEB).

Chiou, B., R. Darragh, N. Gregor and W. Silva (2008). "NGA Project Strong-Motion Database." *Earthquake Spectra* **24**(1): 23-44.

Fenves, G. and M. Scott (2006). "Plastic Hinge Integration Methods for Force-Based Beam–Column Elements." *Journal of Structural Engineering* **32**(2): 244-252.

Ibarra, L., R. Medina and H. Krawinkler (2002). Collapse assessment of deteriorating SDOF systems. *Proceedings of the 12th European Conference on Earthquake Engineering*, London, England, UK.

Kakaletsis, D. and C. Karayannis (2008). "Influence of Masonry Strength and Openings on Infilled R/C Frames Under Cycling Loading." *Journal of Earthquake Engineering* **12**(2): 197-221.

Kakaletsis, D. and C. Karayannis (2009). "Experimental investigation of infilled reinforced concrete frames with openings." *ACI Structural Journal* **106**(2): 132-141.

Kent, D. C. and R. Park (1971). "Flexural members with confined concrete." *Journal of the Structural Division* **97**(7): 1969-1990.

Macedo, L., M. Araújo and J. Castro (2013). Assessment and calibration of the harmony search algorithm for earthquake record selection. *Proceedings of the Vienna Congress on Recent Advances in Earthquake Engineering and Structural Dynamics*.

McKenna, F., G. Fenves and M. Scott (2000). "Open system for earthquake engineering simulation." *University of California, Berkeley, Ca*.

Menegotto, M. and P. Pinto (1973). Method of Analysis for Cyclically Loaded RC Frames Including Changes in Geometry and Non-elastic Behaviour of Elements Under Combined Normal Force and Bending. *Proc., Iabse Symp. Of Resistance and Ultimate Deformability of Structures Acted on by Welldefined Repeated Loads*, Libson, Portugal, International Association of Bridge and Structural Engineering.

Mondal, G. and S. K. Jain (2008). "Lateral stiffness of masonry infilled reinforced concrete (RC) frames with central opening." *Earthquake Spectra* **24**(3): 701-723.

Ohsumi, T., Y. Mukai and H. Fujitani (2016). "Investigation of Damage in and Around Kathmandu Valley Related to the 2015 Gorkha, Nepal Earthquake and Beyond." *Geotechnical and Geological Engineering* **34**(4): 1223-1245.

Paulay, T. and M. J. N. Priestley (1992). Seismic design of reinforced concrete and masonry buildings. Toronto, Ontario, Canada, John Wiley & Sons, Inc.

Petry, S. and K. Beyer (2014). "Scaling unreinforced masonry for reduced-scale seismic testing." *Bulletin of Earthquake Engineering* **12**(6): 2557-2581.

Polyakov, S. V. (1956). Masonry in Framed Buildings : An Investigation into the Strength and Stiffness of Masonry Infilling. "Gosudarstvennoe izdatel'stvo Literatury po stroitel'stvu i arkhitekture", Moscow Russia, (English translation by G. L. Cairns, National Lending Library for Science and Technology, Boston, Yorkshire, England, 1963).

Ricci, P., M. T. De Risi, G. M. Verderame and G. Manfredi (2016). "Procedures for calibration of linear models for damage limitation in design of masonry-infilled RC frames." *Earthquake Engineering &*

Structural Dynamics.

Romão, X., A. A. Costa, E. Paupério, H. Rodrigues, R. Vicente, H. Varum and A. Costa (2013). "Field observations and interpretation of the structural performance of constructions after the 11 May 2011 Lorca earthquake." *Engineering Failure Analysis* **34**: 670-692.

Scott, M. H. and K. L. Ryan (2013). "Moment-Rotation Behavior of Force-Based Plastic Hinge Elements." *Earthquake Spectra* **29**(2): 597-607.

Shakya, M. and C. K. Kawan (2016). "Reconnaissance based damage survey of buildings in Kathmandu valley: An aftermath of 7.8 Mw, 25 April 2015 Gorkha (Nepal) earthquake." *Engineering Failure Analysis* **59**: 161-184.

Vamvatsikos, D. and C. A. Cornell (2002). "Incremental dynamic analysis." *Earthquake Engineering & Structural Dynamics* **31**(3): 491-514.

Zarnic, R. and M. Tomazevic (1988). An experimentally obtained method for evaluation of the behaviour of masonry infilled RC frames. *Proceedings of the 9th World Conference on Earthquake Engineering*, Tokyo-Kyoto, Japan.

Zhai, C., J. Kong, X. Wang and Z. Chen (2016). "Experimental and Finite Element Analytical Investigation of Seismic Behavior of Full-Scale Masonry Infilled RC Frames." *Journal of Earthquake Engineering*: 1-28.